ELSEVIER

Journal of Alloys and Compounds 220 (1995) 53–61

Journal of ALLOYS AND COMPOUNDS

A theoretical study of the phase equilibria in the Cu–Cr–Zr system

K.J. Zeng *, M. Hämäläinen

Laboratory of Materials Processing and Powder Metallurgy, Department of Materials Science and Rock Engineering, Helsinki University of Technology, Vuorimiehentie 2K, SF-02150 Espoo, Finland

Abstract

Small additions of chromium to Cu–Zr alloys or zirconium to Cu–Cr alloys are widely used to improve the mechanical properties of the alloys at high temperatures. There are conflicting opinions in the literature on the question of the existence of the pseudobinary system Cu–Cr_2Zr. From calculation of the Cu–Cr–Zr phase diagram using the CALPHAD method, the possibility of the existence of this pseudobinary has been ruled out. A number of isothermal and vertical sections have been calculated together with the liquidus surface. The reaction scheme for the whole system is also presented.

Keywords: Phase diagrams; Modeling; Thermodynamics; Phase equilibrium; Copper-based alloys

1. Introduction

High conductivity copper alloys which are capable of retaining their high strength after exposure at high temperatures, e.g. during brazing, are of great technical importance. Age-hardened Cu–Cr alloys have good strength and ductility at room temperature and high electrical and thermal conductivities, but they exhibit a severe intermediate temperature embrittlement [1–3]. Although dilute Cu–Zr alloys have shown particular promise in meeting this need [4–7], their strength due to alloying alone is not sufficient. As their desired strength depends on a high level of cold work, strength is lost at high brazing temperatures. Some efforts have been made to improve the overall high temperature properties of these alloys. Sarin and Grant [5] have found that the addition of chromium to Cu–Zr alloys improves the precipitation hardening pronouncedly and results in the best overall properties. Later, Kanno [8] reported that the addition of zirconium to Cu–Cr alloys can improve mechanical properties at high temperatures without impairing the good electrical and thermal conductivities.

These two aspects give rise to the great importance of the Cu–Cr–Zr phase diagram, because from a knowledge of the phase relations and the thermodynamic properties of the phases in an alloy system it is possible to select methods for improving the properties of the alloys and for optimising the production techniques. Unfortunately, such knowledge is not well established for the Cu–Cr–Zr system. Only a few experimental results have been reported. In the available experimental information, there are contradictory results for the phase relations in the Cu-rich corner of Cu–Cr–Zr phase diagram.

The purpose of the present work was to provide an assessment of Cu–Cr–Zr using the CALPHAD method. The method is based on the use of thermodynamic models to describe the Gibbs energy of the various phases in the system. In the models, the thermodynamic data for the pure elements can be taken from the Scientific Group Thermodata Europe (SGTE) database [9], and those for the binary systems can be taken from previous assessments. The ternary parameters must be optimized from experimental information on the ternary system. Once the multicomponent Gibbs energy functions have been obtained, the phase diagram and other interesting thermodynamic quantities may be calculated.

2. Experimental information

There are no experimental thermodynamic data available for the ternary Cu–Cr–Zr system, but some in-

* Present address: Technische Universität Clausthal, AG Elektronische Materialien, Robert-Koch-Strasse 42, D-38678 Clausthal-Zellerfeld, Germany.

SSDI 0925-8388(94)06029-0

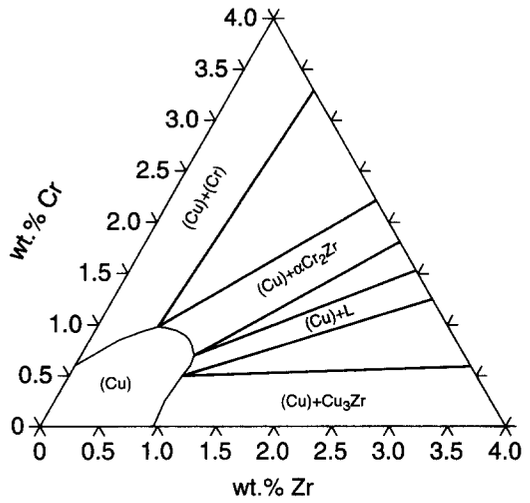

Fig. 1. The isothermal section of the Cu–Cr–Zr equilibrium phase diagram at 940 °C, observed by Zakharov et al. [12].

Table 1
Binary solubilities of Cr and Zr in the (Cu) phase

Cr in (Cu) (wt.%)	Temperature (°C)	Reference	Zr in (Cu) (wt.%)	Temperature (°C)	Reference
0.25	950	[14]	0.11	965	[18]
0.34	970	[16]	0.1	920	[17]
0.33	980	[15]	0.14	925	[19]
0.6	940	[13]	0.9	940	[13]
0.26	950	[20]	0.11	950	[20]

Table 2
Comparison between the observed and calculated invariant equilibria in the Cu–Cr–Zr system

Reaction	Temperature (°C)	Reference
$L + Cu_{51}Zr_{14} \rightarrow Cu_5Zr + (Cr)$	997	[22]
	1001	This work
$L \rightarrow (Cu) + Cu_5Zr + (Cr)$	963	[22]
	963	This work
$L \rightarrow (\beta\text{-Zr}) + \alpha\text{-}Cr_2Zr + CuZr_2$	945	[23]
	966	This work
$(\beta\text{-Zr}) \rightarrow (\alpha\text{-Zr}) + \alpha\text{-}Cr_2Zr + CuZr_2$	814	[23]
	807	This work

formation is available on the phase diagram in the copper-rich and the zirconium-rich corners.

2.1. Cu-rich corner

Glazov et al. [10,11] and Zakharov et al. [12,13] investigated the Cu-rich corner of the Cu–Cr–Zr phase diagram within the composition range up to 3.5 wt.% Cr and 3.5 wt.% Zr by thermal analysis, metallographic analysis and microhardness measurements. Several isothermal and vertical sections were constructed within the temperature range from 600 to 1040 °C, one of which is shown in Fig. 1. A quasi-eutectic reaction $L \rightarrow (Cu) + \alpha\text{-}Cr_2Zr$ was observed to occur at 1020 °C, and therefore a pseudobinary Cu–Cr_2Zr system was supposed.

The boundaries of the solid solution phase (Cu) measured by Glazov et al. [10,11] and Zakharov et al. [12,13] seem to be doubtful because the binary solubilities of Cr in (Cu) and Zr in (Cu) are much greater than the well-established phase diagram data for the binary Cu–Cr [14–16] and Cu–Zr [17–19] systems (Table 1).

The five measured vertical sections of the phase diagram obtained by Zakharov et al. [13] were presented for constant compositions up to 2 wt.% Cr and 2 wt.% Zr, or for 93 wt.% Cu. In a small composition range near pure Cu, two invariant eutectic equilibria, $L \rightarrow (Cr) + (Cu) + \alpha\text{-}Cr_2Zr$ and $L \rightarrow (Cu) + Cu_3Zr + \alpha\text{-}Cr_2Zr$, have been observed at 980 °C and 935 °C respectively. However, the measured liquidus curves in the vertical sections are also doubtful because very great differences exist between the binary liquidus temperatures in these sections and the experimental liquidus data of the binary systems.

Using X-ray diffraction, Kawakatsu et al. [20], Fedorov et al. [21] and Kuznetsov et al. [22] studied the Cu-rich corner of the phase diagram in a wider composition range up to 5 at.% Cr and 20 at.% Zr. Contrary to the work of Glazov et al. [10,11] and Zakharov et al. [12,13], they found no Cr_2Zr phase in their samples. Hence, the pseudobinary system Cu–Cr_2Zr does not seem to exist.

On the basis of metallographic examination, Kawakatsu et al. [20] determined the boundary of the (Cu) phase in the alloys after cold work and solution treatment at 900 and 950 °C. The binary solubilities of Cr and Zr in (Cu) were reported to be 0.26 wt.% and 0.11 wt.% respectively at 950 °C. These values are in very good agreement with the binary phase diagram data (Table 1).

Using metallographic analysis, X-ray diffraction, differential thermal analysis and electron microprobe techniques, Kuznetsov et al. [22] investigated alloys with a constant Cr content (0.5, 1.5 and 5 at.%). No ternary compound was found. Two invariant equilibria, different from those observed by Zakharov et al. [13], were established within a larger composition range in the Cu-rich corner (Table 2). The liquidus projection was constructed on the basis of experimental data and thermodynamic calculations. However, it is not in good agreement with the liquidus of the Cu–Cr binary system.

2.2. Zr-rich corner

The Zr-rich corner of the Cu–Cr–Zr phase diagram (Zr–Cr_2Zr–$CuZr_2$) has been investigated by Tregubov

Table 3
Summary of thermodynamic parameters describing the Cu–Cr–Zr system in SI units (joules, moles and kelvins)

Solution phases: *Redlich–Kister formula* (*referred to* H_i^{SER})

Liquid (parameters with an asterisk optimised in the present work)

${}^{\circ}G_{Cu}^{liq} = 5194.34 + 120.9748T - 24.1124T \ln T - 0.00265684T^2 + 52477.80T^{-1} + 1.292230\times10^{-7}T^3 - 5.83932\times10^{-21}T^7$	$298.15 < T < 1358.02$
${}^{\circ}G_{Cu}^{liq} = -46.90 + 173.8835T - 31.380T \ln T$	$1358.02 < T < 6000$
${}^{\circ}G_{Cr}^{liq} = 15484.0 + 146.060T - 26.9080T \ln T + 0.001894350T^2 + 139250.0T^{-1} - 1.477210\times10^{-6}T^3 + 2.37615\times10^{-21}T^7$	$298.15 < T < 1358.02$
${}^{\circ}G_{Cr}^{liq} = -16459.0 + 335.6180T - 50.0T \ln T$	$1358.02 < T < 6000$
${}^{\circ}G_{Zr}^{liq} = 10320.09 + 116.5682T - 24.16180T \ln T - 0.0043779910T^2 + 34971.0T^{-1} + 1.62750\times10^{-22}T^7$	$298.15 < T < 1358.02$
${}^{\circ}G_{Zr}^{liq} = -8281.260 + 253.8126T - 42.1440T \ln T$	$1358.02 < T < 6000$
${}^{0}L_{Cr,Cu}^{liq} = +35495.913 - 2.957993T$	
${}^{1}L_{Cr,Cu}^{liq} = -1001.1765$	
${}^{2}L_{Cr,Cu}^{liq} = +5704.64789$	
${}^{0}L_{Cr,Zr}^{liq} = -12971.34 + 1.20015T$	
${}^{1}L_{Cr,Zr}^{liq} = +8025.96 - 0.74259T$	
${}^{2}L_{Cr,Zr}^{liq} = -9984.87 + 0.92383T$	
${}^{0}L_{Cu,Zr}^{liq} = -61685.53 + 11.29235T$	
${}^{1}L_{Cu,Zr}^{liq} = -8830.66 + 5.04565T$	
${}^{*0}L_{Cr,Cu,Zr}^{liq} = +62531.693$	
${}^{*1}L_{Cr,Cu,Zr}^{liq} = +69059.941$	
${}^{*2}L_{Cr,Cu,Zr}^{liq} = -71432.450$	

F.c.c.

${}^{\circ}G_{Cr}^{f.c.c.} = 7284 + 0.163T + {}^{\circ}G_{Cr}^{b.c.c.}$	
${}^{\circ}G_{Cu}^{f.c.c.} = -7770.460 + 130.4850T - 24.11240T \ln T - 0.002656840T^2 + 52477.80T^{-1} + 1.292230\times10^{-7}T^3$	$298.15 < T < 1358.02$
${}^{\circ}G_{Cu}^{f.c.c.} = -13542.30 + 183.8040T - 31.380T \ln T + 3.64643\times10^{29}T^{-9}$	$1358.02 < T < 6000$
${}^{\circ}G_{Zr}^{f.c.c.} = -7600 - 0.9T + {}^{\circ}G_{Zr}^{h.c.p.}$	
${}^{0}L_{Cr,Cu}^{f.c.c.} = +88112 - 30.38315T$	
${}^{0}L_{Cr,Zr}^{f.c.c.} = 20000$	
${}^{0}L_{Cu,Zr}^{f.c.c.} = 2233.04$	

B.c.c. (parameters with an asterisk optimized in the present work)

${}^{\circ}G_{Cr}^{b.c.c.} = -8851.930 + 157.480T - 26.9080T \ln T + 0.001894350T^2 + 1.39250\times10^{5}T^{-1} - 1.477210\times10^{-6}T^3$	$298.15 < T < 1358.02$
${}^{\circ}G_{Cr}^{b.c.c.} = -34864.0 + 344.180T - 50.0T \ln T - 2.88526\times10^{32}T^{-9}$	$1358.02 < T < 6000$
${}^{\circ}G_{Zr}^{b.c.c.} = -525.5390 + 124.9457T - 25.60741T \ln T - 3.400840\times10^{-4}T^2 + 2.52330\times10^{4}T^{-1} - 9.7290\times10^{-9}T^3 - 7.61430\times10^{-11}T^4$	$298.15 < T < 1358.02$
${}^{\circ}G_{Zr}^{b.c.c.} = -30705.96 + 264.2842T - 42.1440T \ln T + 1.27606\times10^{32}T^{-9}$	$1358.02 < T < 6000$
${}^{\circ}G_{Cu}^{b.c.c.} = +4017 - 1.255T + {}^{\circ}G_{Cu}^{f.c.c.}$	
${}^{0}L_{Cr,Zr}^{b.c.c.} = +16555.47 + 4.92028T$	
${}^{1}L_{Cr,Zr}^{b.c.c.} = 11365.57$	
${}^{0}L_{Cr,Cu}^{b.c.c.} = 200000$	
${}^{0}L_{Cu,Zr}^{b.c.c.} = -7381.13$	
${}^{*0}L_{Cr,Cu,Zr}^{b.c.c.} = 80496.8$	
${}^{*1}L_{Cr,Cu,Zr}^{b.c.c.} = 80496.8$	
${}^{*2}L_{Cr,Cu,Zr}^{b.c.c.} = 42042.758$	

H.c.p.

${}^{\circ}G_{Zr}^{h.c.p.} = -7827.595 + 125.6491T - 24.16180T \ln T - 0.004377910T^2 + 34971.0T^{-1}$	$298.15 < T < 1358.02$
${}^{\circ}G_{Zr}^{h.c.p.} = -26085.92 + 262.7242T - 42.1440T \ln T - 1.34289\times10^{31}T^{-9}$	$1358.02 < T < 6000$
${}^{\circ}G_{Cr}^{h.c.p.} = +4438 + {}^{\circ}G_{Cr}^{b.c.c.}$	
${}^{\circ}G_{Cu}^{h.c.p.} = +600 + 0.2T + {}^{\circ}G_{Cu}^{f.c.c.}$	
${}^{0}L_{Cr,Cu}^{h.c.p.} = 60000$	
${}^{0}L_{Cr,Zr}^{h.c.p.} = 15791.59$	
${}^{0}L_{Cu,Zr}^{h.c.p.} = 11336.85$	

Laves phase: *sublattice model* (*referred to* G_i^{SER}) (parameters given for 1 mol of sublattice formula)

α-Cr_2Zr: (Cr, Zr)$_2$(Cr, Zr)$_1$

${}^{\circ}G_{Cr:Cr}^{\alpha} = +506.06 + 21.4756T$	
${}^{\circ}G_{Zr:Cr}^{\alpha} = +129697.81 + 4.21443T$	
${}^{\circ}G_{Cr:Zr}^{\alpha} = -81722 + 27.35939T$	
${}^{\circ}G_{Zr:Zr}^{\alpha} = +47469.75 + 10.09822T$	

β-Cr_2Zr: (Cr, Zr)$_6$(Cr, Zr)$_4$(Cr)$_2$ (parameters modified in the present work)

${}^{\circ}G_{Cr:Cr:Cr}^{\beta} = -3100.06 + 83.49948T$	
${}^{\circ}G_{Zr:Cr:Cr}^{\beta} = +255809.25 + 83.49948T$	
${}^{\circ}G_{Cr:Zr:Cr}^{\beta} = -278840.06 + 83.49948T$	
${}^{\circ}G_{Zr:Zr:Cr}^{\beta} = -19930.75 + 83.49948T$	

(*continued*)

Table 3 (*continued*)

γ-Cr_2Zr: (Cr, Zr)$_6$(Cr, Zr)$_4$(Cr)$_2$
$^{\circ}G_{Cr:Cr:Cr}^{\gamma} = +251557.94 - 62.52455T$
$^{\circ}G_{Zr:Cr:Cr}^{\gamma} = +472754.75 - 62.52455T$
$^{\circ}G_{Cr:Zr:Cr}^{\gamma} = +790.68 - 62.52455T$
$^{\circ}G_{Zr:Zr:Cr}^{\gamma} = +221987.44 - 62.52455T$

Cu–Zr compounds: stoichiometric phases (referred to G_i^{SER}) (parameters given for 1 mol of atoms)

Cu_5Zr	$^{f}G = -10299.00$
$Cu_{51}Zr_{14}$	$^{f}G = -12975.58$
Cu_8Zr_3	$^{f}G = -13460.29$
$Cu_{10}Zr_7$	$^{f}G = -14220.59$
CuZr	$^{f}G = -10052.12 - 3.81598T$
$CuZr_2$	$^{f}G = -14634.67 + 1.73017T$

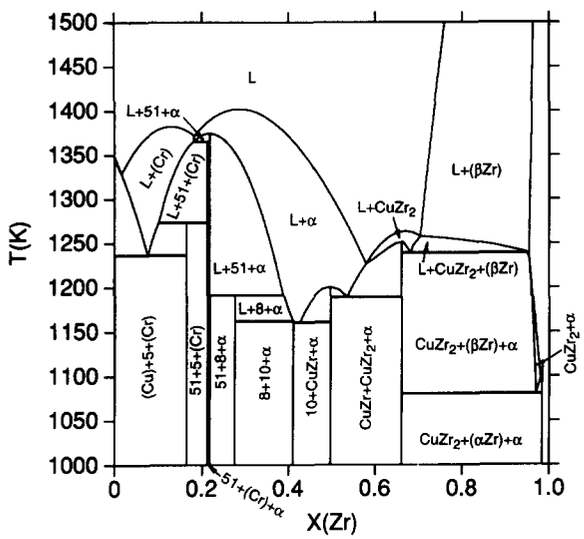

Fig. 2. The calculated vertical section of the Cu–Cr–Zr phase diagram with constant content of 1.5 at.% Cr.

et al. [23] and Malakhova [24]. Using metallographic, thermal and dilatometric analysis, Tregubov et al. [23] constructed two isothermal sections at 750 and 900 °C and a solvus projection of the (β-Zr) phase. No ternary phase was found. A pseudobinary Cr_2Zr–$CuZr_2$ system was supposed. One eutectic and one eutectoid equilibria occur in the Zr-corner at 945 °C and 814 °C respectively (Table 2). Malakhova [24] has constructed isothermal sections at 700 and 875 °C using X-ray analysis. The results confirm the phase relationships reported by Tregubov et al. [23].

3. Thermodynamic models

The Gibbs energies of the pure elements (phase stabilities) vs. temperature $^{\circ}G_i(T)$ were represented by Eq. (1):

$$^{\circ}G_i(T) = a + bT + cT\ln T + dT^2 + eT^{-1} + fT^3 + iT^4 + jT^7 + kT^{-9} \quad (1)$$

The $^{\circ}G_i$ values are referred to the enthalpy of a special standard state, recommended by SGTE [25]. This state, denoted in Table 3 by the superscript SER (for stable element reference), is defined as the stable state at 298.15 K and 0.1 MPa, i.e. f.c.c. Cu, b.c.c. Cr and h.c.p. Zr. The $^{\circ}G_i$ expressions may be given for several temperature ranges, where the coefficients a, b, c, d, e, f, i, j and k have different values. These $^{\circ}G_i(T)$ functions of the pure elements were taken from the work of Dinsdale [9] and are listed in Table 3.

For the composition dependence of G_m of the liquid phase and the terminal solid solutions, the Redlich–Kister [26] formula was used:

$$G_m^{\alpha} = x_{Cu}\,{}^{\circ}G_{Cu}^{\alpha} + x_{Cr}\,{}^{\circ}G_{Cr}^{\alpha} + x_{Zr}\,{}^{\circ}G_{Zr}^{\alpha} + RT(x_{Cu}\ln x_{Cu} + x_{Cr}\ln x_{Cr} + x_{Zr}\ln x_{Zr}) + {}^{E}G_m^{\alpha} \quad (2)$$

where x_i is the mole fraction of the element i; $^{\circ}G_i^{\alpha}$ is the molar Gibbs energy of the element i with the structure of the phase α in a real or hypothetical state and is defined by Eq. (1), and $^{E}G_m^{\alpha}$, the excess Gibbs energy, is treated as follows:

$${}^{E}G_m^{\alpha} = x_{Cu}x_{Cr}L_{Cu,Cr}^{\alpha} + x_{Cu}x_{Zr}L_{Cu,Zr}^{\alpha} + x_{Cr}x_{Zr}L_{Cr,Zr}^{\alpha} + x_{Cu}x_{Cr}x_{Zr}L_{Cu,Cr,Zr}^{\alpha} \quad (3)$$

where $L_{i,j}^{\alpha}$ are binary interaction parameters of the i–j system, which are composition dependent according to the expression

$$L_{i,j}^{\alpha} = \sum_{n=0}^{m} {}^{n}L_{i,j}^{\alpha}(x_1 - x_2)^n \quad (4)$$

where the composition-dependent parameters $^{n}L_{i,j}^{\alpha}$ are generally functions of temperature. The parameter $L_{Cu,Cr,Zr}^{\alpha}$ in Eq. (3) represents the ternary interaction. It is also composition dependent according to the expression

$$L_{Cu,Cr,Zr}^{\alpha} = x_{Cr}\,{}^{0}L_{Cr,Cu,Zr}^{\alpha} + x_{Cu}\,{}^{1}L_{Cr,Cu,Zr}^{\alpha} + x_{Zr}\,{}^{2}L_{Cr,Cu,Zr}^{\alpha} \quad (5)$$

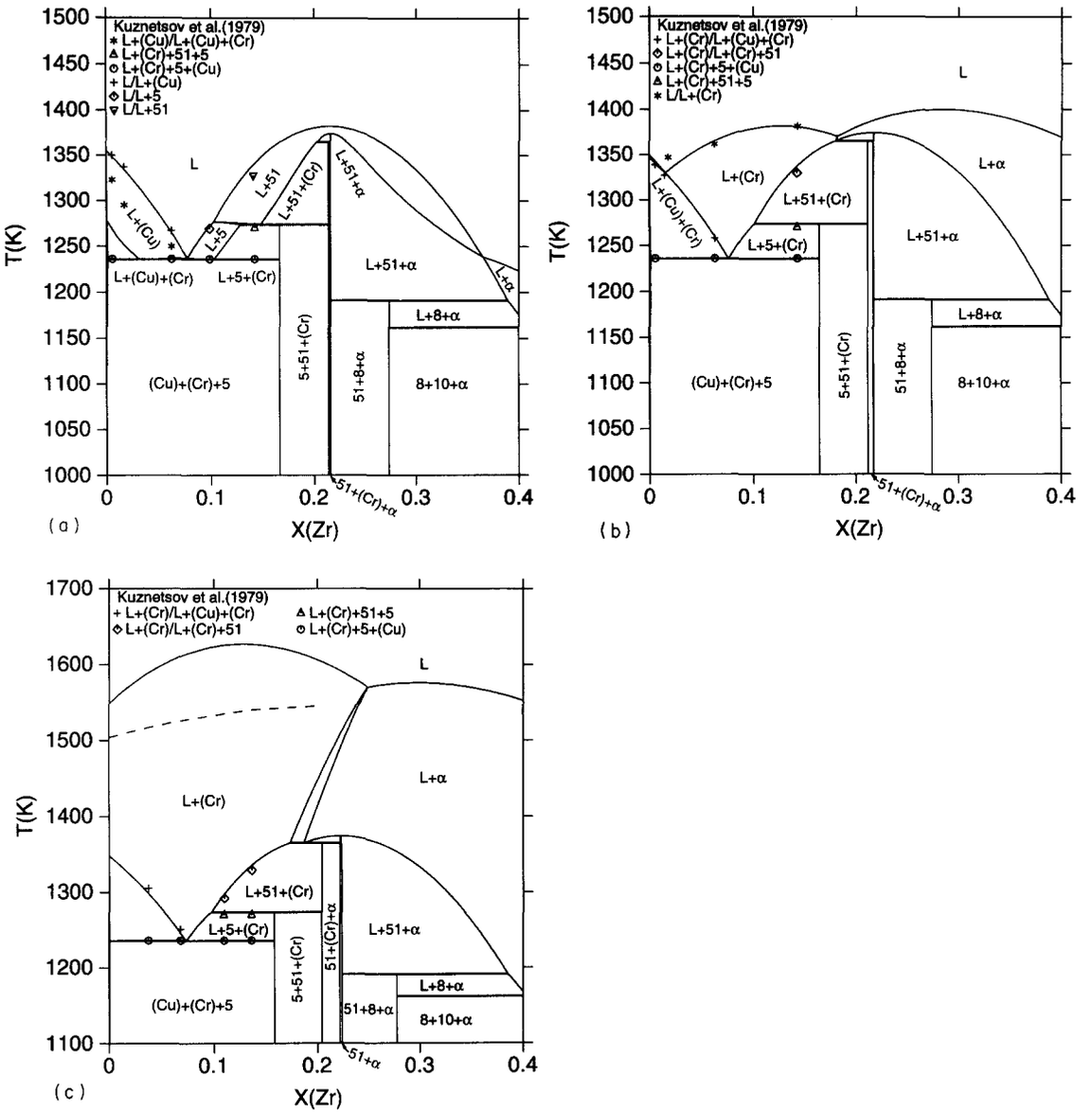

Fig. 3. Comparison between the measured [22] and calculated vertical sections of the Cu–Cr–Zr phase diagram with constant contents of chromium on the Cu-rich side: (a) 0.5 at.% Cr; (b) 1.5 at.% Cr; (c) 5 at.% Cr. The broken curve in (c) is the liquidus line estimated by Kuznetsov et al. [22].

It can only be evaluated from ternary information. The coefficients ${}^{n}L^{\alpha}_{\mathrm{Cr,\,Cu,\,Zr}}$ can also be temperature dependent.

There are three Laves phases in the Cr–Zr binary system and six stoichiometric compounds in the Cu–Zr system. Because no experimental data have been reported for the ternary solubility of the compound phases, they were treated as binary phases.

4. Assessment

As discussed above, the data of Glazov et al. [10,11] and Zakharov et al. [12,13] do not agree with the well-determined phase diagram data for the binary subsystems. Therefore they were omitted from the present work.

The parameters $L^{\alpha}_{\mathrm{i,j}}$ for the solution phases in Eq. (3) were taken from the already optimized binary systems [27–29]. Lacking experimental information for the evaluation of the ternary interaction parameters $L^{\alpha}_{\mathrm{Cu,\,Cr,\,Zr}}$ of the h.c.p. and f.c.c. phases, these were set to zero. For the liquid phase, there are some experimental data on the liquidus surface in the copper corner [22], where temperatures have also been measured for two invariant equilibria [22]. One invariant equilibrium involving the liquid phase (see Table 2) has also been measured in the zirconium corner [23]. It is possible to adjust the ternary parameters of the liquid phase. Because the temperatures of the four

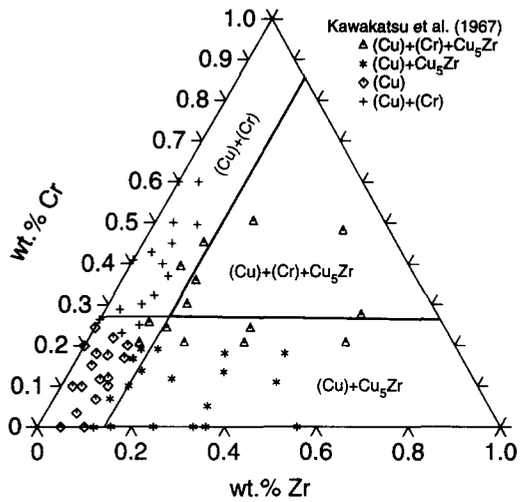

Fig. 4. Comparison between the measured [20] and calculated copper corner of isothermal section of the Cu–Cr–Zr phase diagram at 950 °C.

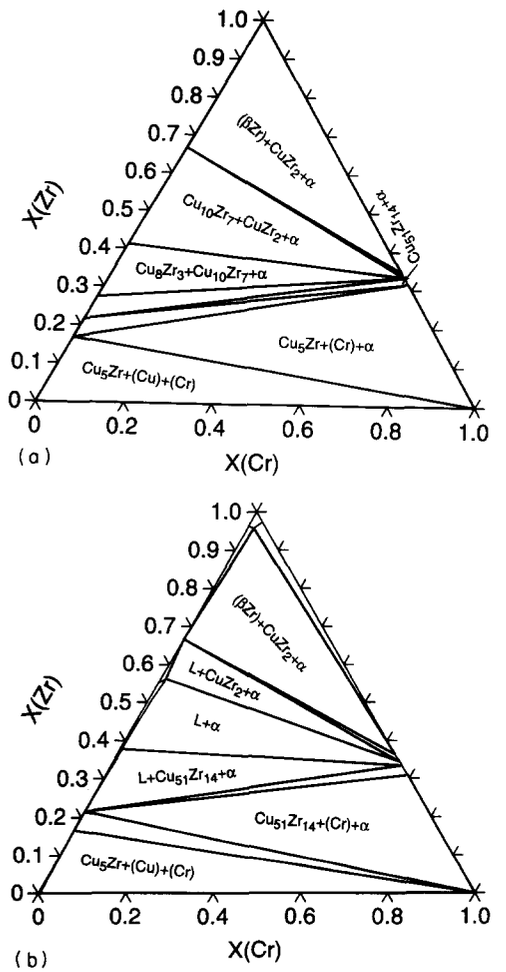

Fig. 5. The calculated isothermal section of the Cu–Cr–Zr phase diagram at (a) 600 °C and (b) 940 °C. α denotes α-Cr_2Zr.

phase equilibria $L \leftrightarrow \alpha\text{-}Cr_2Zr + CuZr_2 + (\beta\text{-}Zr)$ and $(\beta\text{-}Zr) \leftrightarrow \alpha\text{-}Cr_2Zr + CuZr_2 + (\alpha\text{-}Zr)$ have been determined [23], the ternary parameters of the b.c.c. phase

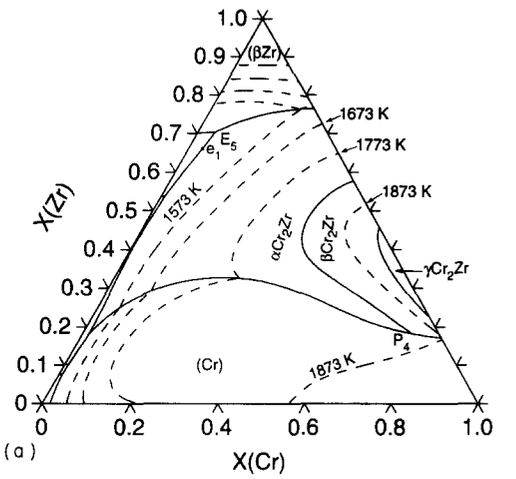

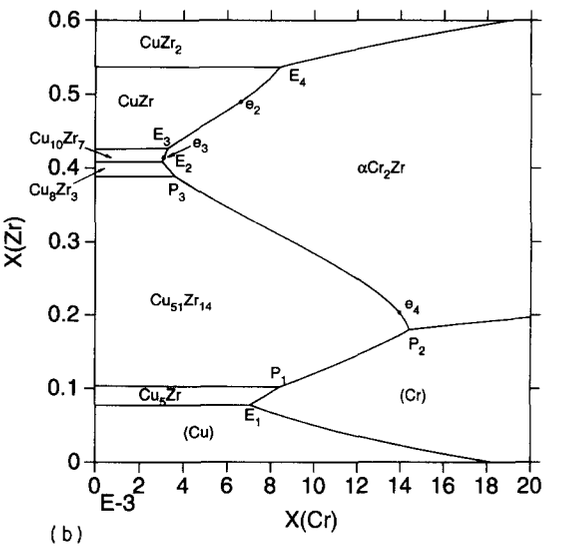

Fig. 6. (a) The calculated liquidus projection of the Cu–Cr–Zr phase diagram. (b) An enlarged part of (a).

can also be adjusted. As no data are available in the chromium corner, ${}^{0}L^{\text{b.c.c.}}_{\text{Cr, Cu, Zr}}$ in Eq. (5) was set equal to ${}^{1}L^{\text{b.c.c.}}_{\text{Cr, Cu, Zr}}$. In the absence of ternary calorimetric data for the liquid and b.c.c. phases, the ternary excess term can be defined only as an excess Gibbs energy. Separation of this term into enthalpy and entropy of mixing contributions must await further experimental work.

The parameters for the binary intermediate phases were taken from the already optimized binary systems [27–29].

5. Results and discussion

Initially, the Cu–Cr–Zr system was calculated without any ternary excess terms in Eq. (3). The ternary diagram thus obtained by simply extrapolating the binary data was very close to the ternary measurements made by Kawakatsu et al. [20] and Kuznetsov et al. [22], except for the liquidus surface, which indicated that the ex-

Table 4
Key points of the liquidus surface projection of the Cu–Cr–Zr system

Symbol	Reaction	Liquid concentration		Invariant temperature (K)
		Cr (at.%)	Zr (at.%)	
E_1	$L \rightarrow Cu_5Zr + (Cu) + (Cr)$	0.706	7.717	1236
P_1	$L + Cu_{51}Zr_{14} \rightarrow Cu_5Zr + (Cr)$	0.8421	10.18	1274
P_2	$L + \alpha\text{-}Cr_2Zr \rightarrow (Cr) + Cu_{51}Zr_{14}$	1.444	18.00	1365
P_3	$L + Cu_{51}Zr_{14} \rightarrow \alpha\text{-}Cr_2Zr + Cu_8Zr_3$	0.3606	38.90	1191
E_2	$L \rightarrow \alpha\text{-}Cr_2Zr + Cu_{10}Zr_7 + Cu_8Zr_3$	0.329	40.88	1161.85
E_3	$L \rightarrow \alpha\text{-}Cr_2Zr + Cu_{10}Zr_7 + CuZr$	0.3275	42.7	1160.6
E_4	$L \rightarrow \alpha\text{-}Cr_2Zr + CuZr + CuZr_2$	0.839	53.71	1189
E_5	$L \rightarrow \alpha\text{-}Cr_2Zr + CuZr_2 + (\beta\text{-}Zr)$	3.948	70.32	1239
P_4	$L + \beta\text{-}Cr_2Zr \rightarrow (Cr) + \alpha\text{-}Cr_2Zr$	75.61	18.25	1820
e_1	$L \rightarrow \alpha\text{-}Cr_2Zr + CuZr_2$	3.187	66.12	1251
e_2	$L \rightarrow \alpha\text{-}Cr_2Zr + CuZr$	0.6464	48.71	1200
e_3	$L \rightarrow \alpha\text{-}Cr_2Zr + Cu_{10}Zr_7$	0.3067	41.14	1161.89
e_4	$L \rightarrow \alpha\text{-}Cr_2Zr + Cu_{51}Zr_{14}$	1.389	20.5	1373

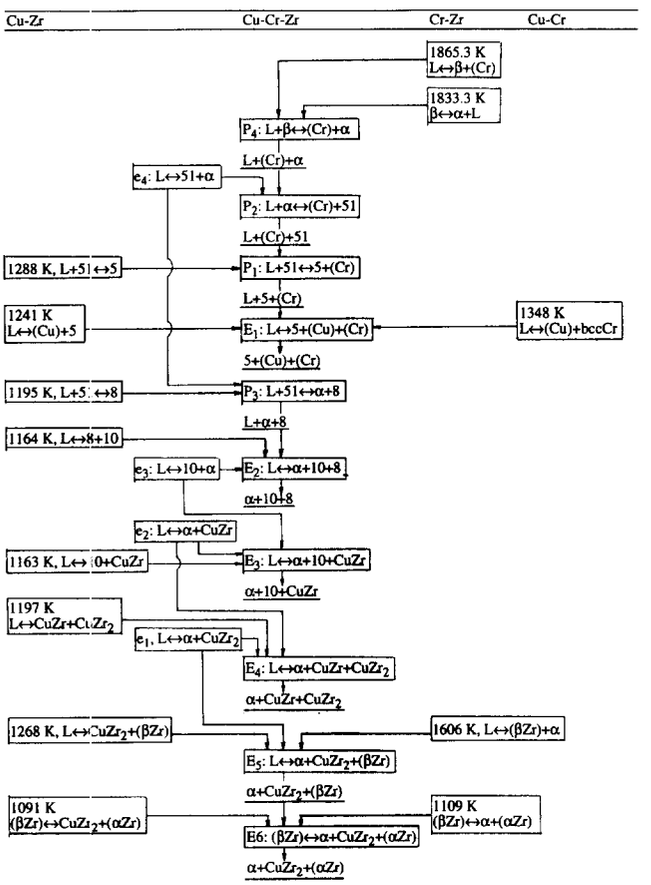

Fig. 7. Reaction scheme of equilibria in the Cu–Cr–Zr system according to the present calculation, where the temperatures for invariant binary reactions are shown. The temperatures for invariant ternary equilibria are listed in Table 4.

perimental results of Glazov et al. [10,11] and Zakharov et al. [12,13] were not consistent with the binary data. Ternary terms as in Eq. (5) were introduced subse-

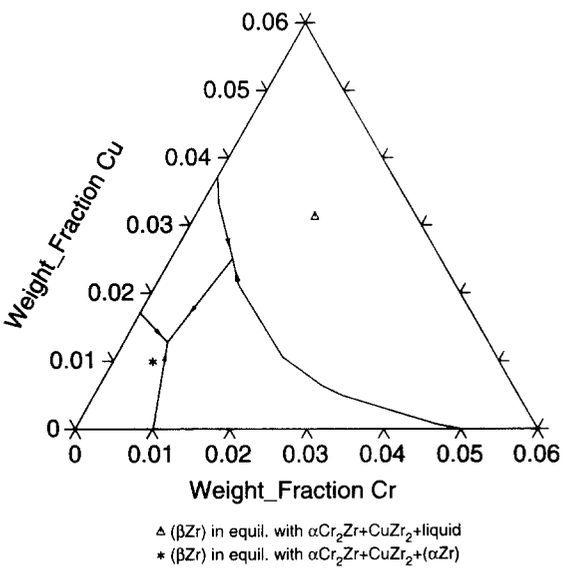

Fig. 8. The calculated solvus projection of the (β-Zr) phase in the Cu–Cr–Zr system.

quently. The optimized ternary parameters are marked with an asterisk in Table 3. Fig. 2 presents a vertical section of the Cu–Cr–Zr phase diagram at 1.5 at.% Cr, calculated with the optimized parameters. For simplicity, the following abbreviations have been introduced in Figs. 2, 3 and 7: α, α-Cr_2Zr; β, β-Cr_2Zr; 5, Cu_5Zr; 51, $Cu_{51}Zr_{14}$; 8, Cu_8Zr_3; 10, $Cu_{10}Zr_7$.

Three calculated vertical sections of the Cu–Cr–Zr phase diagram with constant contents of 0.5, 1.5, and 5 at.% Cr are compared in Fig. 3 with the experimental data of Kuznetsov et al. [22]. A very good fit with the measured data has been obtained (see also Table 2). The calculated liquidus line on the section with constant content of 5 at.% Cr is higher than that estimated by Kuznetsov et al. [22].

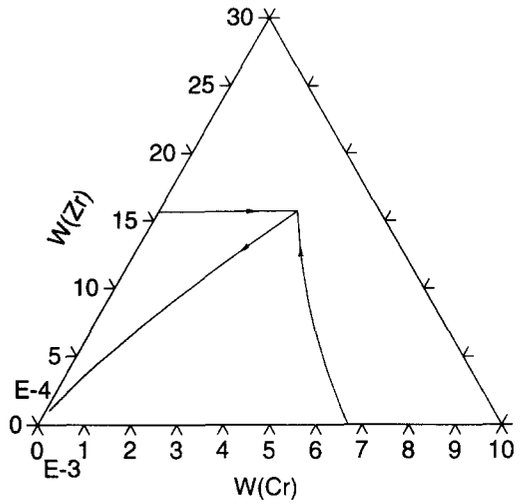

Fig. 9. The calculated solvus projection of the (Cu) phase in the Cu–Cr–Zr system.

The experimental results of Kawakatsu et al. [20] indicate that the addition of zirconium to a Cu–Cr binary alloy will greatly decrease the solubility of Cr in f.c.c. (Cu). However, the optimization showed that a very large ternary interaction parameter, of the order of 10^6, was required for the f.c.c. phase in order to reproduce the f.c.c. phase boundary determined by Kawakatsu et al. [20]. It is the opinion of the present authors that this point should be confirmed by further experimental work, and the Cu corner of the phase diagram at 950 °C has therefore been calculated without an f.c.c. ternary interaction parameter (Fig. 4).

The isothermal sections of the Cu–Cr–Zr phase diagram at 600 and 940 °C are given in Fig. 5. The (Cu) + α-Cr_2Zr two-phase region has not been predicted. The calculated liquidus projection is shown in Fig. 6, with the key points being listed in Table 4. Four quasi-binary eutectic reactions have been predicted (reactions e_1–e_4 in Table 4). These results show that the existence of the pseudobinary Cu–Cr_2Zr system proposed in Refs. [10–13] is not confirmed by the thermodynamic calculation.

Kuznetsov et al. [22] presented the liquidus projection near the Cu–Cr side. The eutectic L ↔ (Cu) + Cu_5Zr + (Cr) was fixed at 0.5 at.% Cr, 7.8 at.% Zr and 963 °C. The calculated values for this equilibrium are 0.71 at.% Cr, 7.7 at.% Zr and 963 °C. The difference in Cr content may be caused by the difference between the observed binary Cu–Cr eutectic composition (with 1.5 at.% Cr) according to Kuznetsov et al. [22] and the calculated composition (with 1.81 at.% Cr) according to Zeng and Hämäläinen [28]. The reaction scheme for the equilibria in Fig. 6 is presented in Fig. 7, where the temperatures for invariant binary reactions are shown, and those for the invariant ternary equilibria are listed in Table 4.

Fig. 8 illustrates the projection of the solvus surface of b.c.c. (β-Zr). The eutectoid reaction (β-Zr) ↔ α-Cr_2Zr + $CuZr_2$ + (α-Zr) is predicted to occur at 0.568 wt.% Cr, 1.276 wt.% Cu and 1080 K, which is in good agreement with the measurements made by Tregubov et al. [23]. However, the calculated temperature of the eutectic reaction L ↔ α-Cr_2Zr + $CuZr_2$ + (β-Zr) is 21 K higher than the value measured by Tregubov et al. [23] (Table 2). The calculated equilibrium concentration of (β-Zr) at the eutectic temperature is also not in agreement with observation. Lacking experimental data on the liquidus and solidus surfaces of (β-Zr), no further attempt was made to improve the fit.

Fig. 9 shows the projection of the solvus surface of f.c.c. (Cu). The maximum solubility of this phase is 0.299 wt.% Cr and 0.157 wt.% Zr at 1236 K.

Acknowledgements

The authors are grateful to Professor K. Lilius for providing excellent working conditions in his laboratory. Special thanks are due to Dr. P. Taskinen in Outokumpu Research Centre of Finland for useful advice.

References

[1] M.J. Saarivirta and P.P. Tabenblat, *Trans. Metall. Soc. AIME, 218* (1960) 935–939.
[2] H. Suzuki, M. Kanno and H. Kitano, *J. Jpn. Inst. Met., 34* (1970) 497–501.
[3] S. Sato, T. Otsu and E. Hata, *J. Inst. Met., 99* (1971) 118.
[4] A.V. Nadkarni and E.P. Weber, *Weld. J., 56* (1977) 331–338.
[5] V.K. Sarin and N.J. Grant, *Powder Metall. Intr., 11* (1979) 153–157.
[6] E. Ling and P.W. Taubenblat (eds.), *High Conductivity Copper and Aluminium Alloys*, Metallurgical Society, Warrendale, PA, 1984.
[7] W.C. Shumay, Jr., *Adv. Mater. Proc. Inc. Met. Prog., 132* (1987) 54–60.
[8] M. Kanno, *Z. Metallkd., 10* (1988) 687.
[9] A.T. Dinsdale, *Calphad, 15* (1991) 317–425.
[10] V.M. Glazov, M.V. Zakharov and M.V. Stepanova, *Izv. Akad. Nauk SSSR, Otdl. Tekh. Nauk*, (1) (1956) 162–164.
[11] V.M. Glazov, M.V. Zakharov and M.V. Stepanova, *Izv. Akad. Nauk SSSR, Otdl, Tekh. Nauk*, (9) (1957) 123–126.
[12] M.V. Zakharov, M.V. Stepanova and V.M. Glazov, *Metalloved. Term. Obrab. Metall.*, (3) (1956) 23–27.
[13] M.V. Zakharov, M.V. Stepanova and V.M. Glazov, *Metalloved. Term. Obrab. Metall.*, (3) (1957) 23–27.
[14] T. Doi, *J. Jpn. Inst. Met., 21* (1957) 337.
[15] M.V. Zakharov and O.E. Osintsev, *Izv. Vyssh. Ucheb. Zaved., Tsvetn. Metall.*, (5) (1967) 152–155.
[16] W.R. Hibbard, Jr., F.D. Rosi, H.T. Clark, Jr., and R.I. O'Herron, *Trans. AIME, 175* (1948) 283.
[17] M.J. Saarivirta, *Trans. Metall. Soc. AIME, 218* (1960) 431–437.
[18] U. Zwicker, *Metall (Berlin), 16* (1962) 409–412.
[19] W. Showak, *Trans. Metall. Soc. AIME, 224* (1962) 1297–1298.
[20] I. Kawakatsu, H. Suzuki and H. Kitano, *Nippon Kinzoku Gakkaishi, 31* (1967) 1253–1257.

[21] V.N. Fedorov, M.V. Zakharov, O.E. Osintsev and V.I. Kucherov, *Zr. Fiz. Khim., 46* (1972) 181–182.

[22] G.M. Kuznetsov, V.N. Fedorov, A.L. Rodnyanskaya and E.A. Naumova, *Izv. Vyssh. Ucheb. Zaved., Tsvetn. Metall.,* (1) (1979) 95–98.

[23] I.A. Tregubov, L.N. Evseeva and O.S. Ivanov, *Izv. Akad. Nauk SSSR, Met.,* (5) (1977) 228–231.

[24] T.O. Malakhova, in O.S. Ivanov and Z.M. Nauka (eds.), Splavy At. Energ., Vol. 5, Moscow, 1979, pp. 123–130.

[25] M. Hillert, in L.H. Bennett (ed.), *Computer Modelling of Phase Diagrams,* Metallurgical Society of AIME, Warrendale, PA, 1986, pp. 1–17.

[26] O. Redlich and A.T. Kister, *Ind. Eng. Chem., 40* (1948) 345–348.

[27] K. Zeng, M. Hämäläinen and R. Luoma, *Z. Metallkd., 84* (1993) 23–28.

[28] K. Zeng and M. Hämäläinen, *Rep. TKK-V-B87,* 1993 (Helsinki University of Technology).

[29] K. Zeng, M. Hämäläinen and H.L. Lukas, *J. Phase Equilib.,* in press.